Two-Photon Calcium Imaging of Evoked Activity from L5 Somatosensory Neurons in vivo.

Wolfgang Mittmann, Damian Wallace, Uwe Czubayko, Jan Thomas Herb, Andreas T. Schaefer, Loren Looger, Winfried Denk, Jason N D Kerr

Two-Photon Calcium Imaging of Evoked Activity from L5 Somatosensory Neurons *in vivo*.

Wolfgang Mittmann[1,2], Damian J. Wallace[1], Uwe Czubayko[1], Jan T. Herb[3], Andreas T. Schaefer[3], Loren L. Looger[4], Winfried Denk[2], and Jason N. D. Kerr[1,5]

[1]Network Imaging Group, Max Planck Institute for Biological Cybernetics, Spemannstraße 41, 72076 Tübingen, Germany.

[2]Department of Biomedical Optics, Max Planck Institute for Medical Research, Jahnstraße 29, 69120 Heidelberg, Germany.

[3]Behavioural Neurophysiology, Max Planck Institute for Medical Research, Jahnstraße 29, 69120 Heidelberg, Germany.

[4]Howard Hughes Medical Institute, Janelia Farm Research Campus, Ashburn, Virginia, USA.

[5]Correspondence to:

Jason Kerr

Network Imaging Group

Max Planck Institute for Biological Cybernetics

Spemannstraße 41 72076 Tübingen Germany

Phone: +49 (0)7071 6011721

Fax : +49 (0)7071 6011720

email: jason@tuebingen.mpg.de

Abstract

Multiphoton imaging is widely used for recording activity simultaneously from many neurons in superficial cortical layers *in vivo*. Here we combine regenerative amplification multiphoton microscopy (RAMM) with genetically encoded calcium indicators to extend multiphoton imaging of neuronal population activity into layer 5 of adult mouse somatosensory cortex. We show that this approach can be used to record and quantify spontaneous and sensory-evoked activity in populations of layer 5 neuronal somata located as much as 800μm below the pia. In addition, we show that RAMM can be used to simultaneously image activity from large (~80) populations of apical dendrites and follow these dendrites down to their somata of origin.

Introduction

Multiphoton imaging (MPI)[1] has been instrumental in measuring spatial and functional organization of neuronal populations in the primary sensory[2-5] and motor cortices[6]. Imaging activity in neuronal populations allows the unambiguous assignment of recorded activity to a neuronal soma and the spatial mapping of activity from all neurons in a local area, especially those firing action potentials at low rates[7]. In addition, the spatial locations of neuron somata can be measured with respect to other neurons in a population and to the cortical layering pattern[2-5,6]. MPI is well suited for imaging either genetically encoded[8-10] or chemically synthesized (for recent review see ref: 11) activity indicators in both anesthetized and awake animals[12,13]. Even though activity in dendrites of individually filled deep-layer neurons has been imaged[14], imaging activity in populations of neuronal somata has been largely restricted to superficial cortical layers[3,15-17]. The main reason for this depth limit is the attenuation of the excitation light by scattering in cortical tissue. Scattering can be reduced by using longer excitation wavelengths[18], but currently no suitable activity indicators exist for those wavelengths. Imaging depth can be increased - to a point - by increasing the average excitation power and thereby MP excitation[19]. Alternatively one can increase the efficiency of MP excitation (at a given average power) by optically amplifying a selected subset of laser pulses[20], using a regenerative amplifier, which results in a train of pulses at reduced repetition frequency but higher energy per pulse. Using a regenerative amplifier operated at a repetition frequency of 200 kHz, GFP-labeled cortical cells could be visualized down to ~1000 µm below the pia[20], at an average laser power of ~45mW at the surface. This suggests that it might also be possible to image functional signals at such depths. Functional imaging,

however, requires frame rates of around 10 Hz (for review see ref: 21), and to date, has been restricted to < 400 μm in depth. Another fundamental limitation to imaging depth is fluorescence from the upper cortical layers, which is particularly serious for homogeneously labeled tissue[19]. For this reason, image quality at increased cortical depths should be improved by sparsely labeling preparations in a way that minimizes staining of upper-layer cortical neuropil (for an example see ref: 7). In the current study we combined RAMM with sparse labeling of deep neurons using the recently developed genetically encoded calcium indicator GCaMP3[9] and show that functional signals (Ca^{2+} transients) can be recorded from somata and apical dendrites of cortical layer 5 (L5) neurons in adult mouse somatosensory cortex *in vivo*.

Results

We used a setup previously described by Theer *et al.* (2003) (**Fig. 1a**). The excitation source for the MP microscope was a regenerative amplifier (RegA 9000, pumped by a 10W Verdi, seeded with sub-sampled pulses from a Mira 900-F pumped by a 5W Verdi; all from Coherent, Dieburg, Germany). The RegA was modified to operate at 925 nm. At this wavelength GFP is more efficiently excited and scattering and intrinsic fluorescence are reduced compared to the RegA's standard operating wavelength of 800 nm[19]. Pulsing of the regenerative amplifier was synchronized with the microscope's image acquisition pixel clock via a custom made circuit[22]. This allowed the output pulses from the RegA to be timed such that the excitation light for each pixel consisted of one pulse from the amplifier delivered near the beginning of the pixel integration time. This limited the pixel rate at most to 200 kHz (all functional images were recorded with a rate of 70 kHz). Fluorescence collection and resolution were further optimized by using a high-numerical-aperture objective lens (Zeiss W Plan-Apochromat, 20x/1.0 NA DIC VIS-IR). To efficiently capture the fluorescence light[23], almost all of which is multiply scattered and emerges diffusely from the sample across an area that increases in diameter as the imaging depth increases, we used a large aperture detection system[2,7,23]. The pulse width after the objective was ~157 fs (after optimizing the GVD). For imaging, deep layer cortical neurons in mouse somatosensory cortex were labeled with GCaMP3 delivered using an adeno-associated virus (AAV) vector[9]. Virus injections were targeted stereotactically to the primary somatosensory cortex and were made using long tapered glass capillaries at cortical depths ranging from ~650-1000 μm. Mice were between 19 to 23 days old (between 8.2 and 10 g, n=12 animals) at the time of the initial virus injection;

the expression time ranged from 10 to 54 days (mean 28 days, n=11 animals). The pipette penetration angle was set to ~28º from the horizontal, which meant that the pipette entry point into the cortex was 1-1.5 mm from the eventual site of imaging. This procedure minimized damage to the cortical tissue overlying the labeled neurons. Typically, a few hundreds of neurons were labeled between 580 and 800 μm below the pia (**Fig. 1b-d, Supplementary Movie 1**), corresponding to cortical L5a and L5b. Targeting to L5 was confirmed by *post hoc* histological staining of the loaded region with DAPI stain (**Fig. 1d,** see **Supplementary Fig. 1**). Neuronal somata could be clearly seen in deep cortical layers and their apical dendrites could be followed easily up to layer 1 (**Fig. 1b**) where astrocytes were brightly stained with Sulforhodamine 101 (**Supplementary Fig. 1b**)

The key to imaging neuronal activity in deeper cortical layers is sufficient contrast and signal in each imaging frame, while imaging at frame rates sufficient for the detection of Ca^{2+} transients[21]. To test this, we recorded continuous datasets using 64 × 64 pixel frames at a rate of 15.6 Hz (1 ms per scan line) from labeled L5 neuronal somata while simultaneously deflecting multiple mystacial whiskers using a small mesh attached to a piezo plate. Ca^{2+} transients in L5 neuronal somata were detectable as deep as 800 μm (**Fig. 2a-f, supplementary Fig. 2**). In general, transients were larger in the apical dendrite than in the soma (**Fig 2c**). Ca^{2+} transients synchronized with sensory stimulation were clearly visible both in apical dendrites and in neuronal somata (**Fig. 2e**) as much as 800 μm below the pia (**Fig. 2f**). Although nuclear exclusion diminished with longer indicator expression times, neurons without clear nuclear exclusion displayed stimulus-evoked calcium transients very similar to those with shorter expression times.

Whether Ca^{2+} transients are caused by action potentials in a given GCaMP3-labeled soma, or are due to contamination by a signal originating from labeled neuropil surrounding the soma of interest[7] depends on axial resolution[21] can be estimated by using linear regression[13,24] (see methods). We found that while in our preparations there was also a strong signal in the neuropil around the somata of layer 5 neurons (**Fig. 2d**), the neuropil contamination of the somatic signal was small (absolute value 0.49% ± 0.06% ΔF/F0, n = 9 neurons, 800μm below pia) compared to the fluorescence increases (~10%, **Fig. 2e**) associated with discharge of evoked APs.

Next we tested whether signals from deep somata are contaminated by signals from probe molecules located in overlying layers, given that such signals become more likely as the excitation power needs to be increased with depth[22]. Because signal generation in superficial layers does not depend much on the lateral position of the focus, the presence of such signals would lead to a correlation between the somatic and neuropil signals that increases with depth[7]. Because this was not observed (regression $1.0x10^{-4}$ ± $9.1x10^{-5}$ S.E, not significantly different from 0, Student's t-test) we conclude that somatic Ca^{2+}-transients recorded from layer 5 neurons *in vivo* are not significantly contaminated by signals from surrounding or superficial neuropil. Finally, to quantify and compare image contrast at different imaging depths, we measured the ratio between the average resting fluorescence in the soma (So) and that in a ring-like annulus ~3 pixels wide around (Su) the soma (So/Su ratio) for each imaging frame and found that the contrast changes only little with depth (**Supplementary Fig. 3**).

Using a thresholding method[6] to identify responses to the presentation of sensory stimuli[10], we found a response rate of 0.24 ± 0.12 Ca^{2+} transients per stimulus (mean ±

SD, 135 neuronal somata and dendrites in 6 fields of view, n=3 animals). This was slightly, but not significantly, higher than that reported for L2/3[2] (P = 0.48, wilcoxon rank sum test) and is consistent with stimulus-evoked firing rates found in layer 5 pyramidal neurons in barrel cortex under anesthesia, under the assumption that the imaged population is a mixture of both thin-tufted and thick-tufted pyramidal neurons, which have response rates of 0.15 and 0.35 APs/stim, respectively[25].

Because L5 is thought to generate a major fraction of all spikes in the whole column per whisker stimulus[26] but shows a wide range of response probabilities[25,26], we calculated the response probability for each neuron and the correlations between neurons within the population. We found a wide range (from 0 to 0.55) of response probabilities (Fig. 2g). The average correlation between pairs of neurons was low, but varied considerably across pairs (0.14 ± 0.22, mean ± SD, 1668 pairs, **Fig. 3a**). Under anaesthesia, the pairwise correlations during spontaneous activity depend on firing rates both *in vivo*[13] and *in vitro*[27]. We therefore tested whether such a relationship holds within layer 5 during evoked activity and found that the strength of pairwise correlations increased strongly with the mean evoked firing rates of L5 neurons (**Fig. 3b,c**). Given the large range of correlations seen between neurons within a local population, we suspected that local synchrony occurs across a population that involves more than a few neurons from one trial to the next. To test this we determined how the fraction of neurons that were active varied from trial to trial[2] taking all neurons in the field of view as a single population. We found that the fraction of neurons responding to one whisker stimulation varied widely (from 0 to 0.93) with the likelihood of large, population-wide responses far

exceeding what is expected for the case where neurons within a population fire independently, each with its measured response probability (**Fig. 3d**) .

RAMM allows the recording of Ca^{2+} transients in the somata of these L5 neurons, but to record activity from all neuronal somata in an area, imaging in multiple focal planes is necessary. This can be avoided by placing the focus at an intermediate depth (e.g. L1-4) and recording from all apical dendrites passing through this plane. Importantly, the correct assignment of activity recorded in a dendritic branch to the soma of origin is achieved by following the dendrites down to their respective somata located in deeper layers (**Fig 4 a-c, Supplementary video 1**). Apical dendrites of L5 pyramidal neurons support back-propagating action potentials *in vitro*[28] and *in vivo*[14] and are an important site for coincidence detection and for the integration of activity from local and remote cortical regions[29,30]. *In vitro,* such back-propagating APs can initiate regenerative dendritic spikes[31] but it is not clear whether, or how this operates *in vivo.* In particular, it is unclear whether all upper-level branches are invaded. Accordingly, we recorded as many as 80 dendrites simultaneously in a single imaging field-of-view in the superficial layers (~100-200 μm below the pia, see **Supplementary Fig. 4**). We found groups of up to 4 branches to have tightly synchronized spontaneous Ca^{2+} transients (**Fig. 4b,c** and **Fig. 5b** grey box). It is, however, not discernable from a single plane whether groups of synchronized branches belong to the same neuron or whether they reflect synchronization between different neurons. To resolve this, we followed the branches downward using the z-stacks we had taken and then traced them, wherever possible, back to their somas of origin (~60 out of a total of 80, n = 5 animals, See Supplementary Movie 1). We then assigned recorded dendritic Ca^{2+} transients to those somas (**Fig. 5a**). In some cases,

several superficial branches having synchronous activity could be traced back to a single branch-point and finally back to the soma of origin, allowing for an unambiguous identification of the dendrite as belonging to a L5 neuron (**Fig. 5 a-d**). Whenever activity was observed in one sub-branch of an apical dendrite, it was observed in all other co-imaged sub-branches (**Fig**. **5b**,**d,** and **Supplementary Fig**. **5**). The axial resolution was not noticeably degraded as basal dendrites belonging to the labeled neuronal somata were often seen (**Fig**. **5h**). Note, that the functional imaging of the apical dendrites at the superficial plane could alternatively be performed using a conventional pulsed Ti:Al_2O_3 laser, which, due to the much higher pulse repetition rate, would allow higher pixel numbers in a single frame without a reduction of the frame rate. The RAMM approach could subsequently be used for purely anatomical imaging down to deep layers. RAMM may also extend the depth range of two-photon targeted patching[32] but the shallow approach angle needed for the pipette to avoid contact with the large diameter objective lens is a potential problem.

Discussion

We have presented a method that extends MP activity imaging to a large fraction of the cortical column. We have shown that it is possible to record sensory evoked transients from large populations of L5a and L5b neurons and measure correlated activity on a single trial basis. We show that pairwise correlations in L5 neurons are low, but that large, correlated responses across the local population occur in response to whisker stimulation similar to what has been reported for L2/3 neuronal populations[2]. We have shown that it is possible to resolve and record from large populations of neuronal

dendrites and unambiguously assign their activity to their somata of origin. Using this approach, activity from the deepest cortical layer, currently out of reach, could, in principle, be recorded by imaging the apical dendrites from L6 cells as they pass through L4. Finally, we provide evidence that activity propagates equally into all apical branches of L5 neurons *in vivo*. As activity indicators for longer wavelengths become available, the use of such wavelengths becomes attractive to further increase depth penetration[18], both at high repetition rates or using the RAMM approach. Spherical aberration, which is caused by the refractive index mismatch between brain tissue and the immersion solution and increases with depth, may need to be corrected using appropriate optics[33] to prevent loss of resolution and excitation. Higher order and/or time-varying aberrations could be corrected using adaptive optics[34,35]. Combining all these approaches will most likely allow imaging all the way to the white matter.

Author contributions: WM DJW WD JNDK designed the research, WM DJW JNDK performed the research, DJW JNDK analyzed the data, UC performed the histological reconstructions, and JTH ATS LL produced the virus, WM DJW JNDK WD wrote the manuscript.

Acknowledgements:
We would like to thank: Patrick Theer for technical help with the RegA, George Sawinski for help with detection system fabrication, David S. Greenberg for dendrite morphology analysis. Supported by the Max Planck Society.

Figure legends:

Figure 1. Imaging L5 Somatosensory cortex neurons labeled with GCaMP3. (**a**) Basic optical path of the microscope and the regenerative amplifier (RegA) seeded by a pulsed Ti:Al_2O_3 laser source (Mira). Pulses from the source laser were subsampled and amplified within the RegA (not to scale) and dispersion compensated (not shown). The pulses entered the microscope at a pixel frequency of <200 KHz, whereas the pulses entering the regenerative amplifier had a frequency of ~76 MHz. (**b**) Two-photon microscope image (side projection) from a z-stack (2 μm steps). L5 neurons labeled with GCaMP3 (green) in an anesthetized mouse. (**c, d**) *Post mortem* fixed tissue slice imaged using widefield-fluorescence. Note staining of axons spreading to thalamus and to contralateral cortex. (**d**) Higher resolution and additional staining with DAPI (Blue) showing cortical layers and corpus collosum (cc).

Figure 2. Sensory stimulation-evoked calcium transients from populations of L5 somata and dendrites, *in vivo*. (**a,b**) Somata and dendrites imaged at two different depths within L5 (distances below pia are as indicated, scale bars are 20 μm). (**c**) Calcium transients recorded from a soma (yellow circle) and 2 dendrites (red, blue circles) at 680 μm below pia during whisker stimulation (blue stripes, yellow circle denoted trace from neuron in **a**, blue and red colored circles indicate corresponding dendrites). (**d**) Calcium transients recorded from 3 somata and neuropil (blue) at 740 μm below the pia during whisker stimulation, neuropil trace averaged across the space between neurons in the entire frame (numbers refer to neurons in **b**). (**e**) Single transients (grey) and their average (black) from L5 neuronal somata (left) dendrites (right) in response to whisker stimulation

(arrow). The left upper panel shows 11 individual traces recorded from a neuronal soma at 630μm below the pia and meeting the criteria for stimulus-evoked Ca^{2+} transients (see Methods). Lower panel shows 12 individual traces determined by the same criteria as response failures. The right panel shows 9 responses (upper) and 15 failures (lower) traces recorded from a dendrite 537 μm below the pia. (**f**) Single transients (7 traces shown, grey) and their average (black) recorded from L5 somata in response to whisker stimulation (arrow) at 800μm below the pia. (**g**) Distribution of response rates.

Figure 3. Layer 5 activity correlation structure. (**a**) Distribution of evoked pairwise correlations. (**b**) Pairwise correlation matrix for all neuronal pairs ranked by response rate (lowest, top left, to highest, bottom right) for a single population. (**c**) Correlation of stimulus evoked firing in neuronal pairs compared to their response rate (geometric mean, bars depict standard error, n = 6 populations). (**d**) Mean distributions of the fraction of neurons in the population that is active during each trial (green) and the distributions expected for independent firing (black).

Figure 4. Measuring activity in populations of dendrites. (**a**) Overview taken at the border of L1 and L2, 200 μm below the pial surface, showing GCaMP3 labeled dendrites and several superficial neuronal somata from L2 neurons (arrows). (**b**) Activity simultaneously recorded from multiple apical L5 neuronal dendritic branches passing through the image plane. (**c**) Overlaid transients from different dendrites (i and ii, same traces as in **b**).

Figure 5. Spontaneous activity in dendrites and its identification with the originating somata. (**a**) y-z side projection from a z-stack taken at 2 μm steps showing multiple L5 neurons and ascending apical dendrites containing GCaMP3 (left) with individual x-y frames from three different depths, indicated by white dashed lines on the y-z projection. (**b**) Calcium transients from three separate dendrites indicated in **a.** Note similarity between transients (grey box). (**c**) Calcium transient recorded from the apical dendrite closer to the soma (bottom image, arrow). (**d**) Reconstructed apical dendrite showing common source of dendritic activity shown in **e** (branch colors correspond to colors in **b**) and **c**. Location of recordings indicated by dashed lines. (**e**) Image taken at 800 μm below pia showing basal dendrites (arrow heads).

Methods:

Microscope Setup

Multiphoton *in vivo* imaging was performed on a custom built microscope using a regenerative amplifier as the source of excitation light as described in[20]. More specifically, the source of excitation light was a regenerative amplifier (RegA 9000, Coherent, Dieburg, Germany) pumped by a 10W Verdi (Coherent, Dieburg, Germany) and seeded with sub-sampled pulses from a conventional TiAl2O3 laser (Mira 900-F pumped by a 5W Verdi, Coherent, Dieburg, Germany). The RegA was modified to operate at a center wavelength of 925 nm to optimize excitation of green fluorescent protein, and to reduce scattering and auto-fluorescence excitation in cortical tissue. To suppress the amplification of spontaneous emission, the flat cavity mirror M6 of the RegA was replaced with a 890 nm cut-off long-pass mirror (Chroma, VT, USA). The RegA light pulses had a duration of ~157 fs after GVD compensation with an average power of 280 mW at a frequency of 200 kHz or 1.5 10^{-6} J/pulse, compared to 2,8 10^{-9} J/pulse of the seeding laser. Pulse repetition rate was minimized by synchronizing the pulses from the RegA with the pixel clock of the acquisition system, such that the output of the RegA was timed to coincide with the beginning of the pixel integration time. The pixel frequency varied depending on the desired pixel dimensions and frame rate of the image. We commonly used repetition frequencies between ~70 and ~160 kHz (lines containing 54 – 256 pixels at 1-2 ms per line). The intensity of the excitation light was controlled using a Berek compensator, with a glan-laser-prism serving as the analyzer (for details see: W. Denk US patent No. 6,249,379 B1 (2001)). A high numerical aperture 20x objective (Zeiss W Plan-Apochromat, 20x/1.0 NA DIC VIS-IR) was used for all data

acquisition. The detection system was as described in[7] and was a custom design with large apertures[23].

Animal preparation

All procedures were conducted according to the animal welfare guidelines of the Max Planck Society and the state of Baden Wurttemberg, Germany. Throughout all procedures body temperature was maintained around 37ºC using a regulated heating blanket and rectal thermal probe. Eleven C57BL/6 mice (Charles River, Germany) ranging in age from 10 to 54 days on the day of the initial virus injection were used for the current study. Anesthesia was induced with ketamine and xylazine (120mg/kg and 5mg/kg, Ketamine from WDT, Germany; xylazine (Rompun) from Bayer, Germany), and maintained using supplementary doses between 10 and 20% of the induction dose whenever the animal began to recover withdrawal reflexes. The bone overlying the left somatosensory cortex was exposed. After identifying the location of the whisker representation in the somatosensory cortex (1.5 mm caudal from bregma, left lateral 3 mm), a small craniotomy (approx. 0.5 x 0.5 mm) was performed 1.5-2 mm posterior to that location and the dura mater was removed. A long-taper glass pipette (tip beveled at 30º, using a BV-10 (Sutter Instruments, Novato, USA) inner diameter 8-15 μm) was filled with the GCaMP3 virus stock solution. The pipette tip was first placed on the surface of the cortex in a location clear of surface blood vessels and was then advanced by 1.3 to 1.8 mm along the axis of the pipette. As the axis was at an angle of 27.5º from the horizontal this places the tip of the pipette at a depth of 650-900 μm in the target area. Virus injections ranged in volume between 50 and 150 nl; the virus solution was injected

at 2-7 psi over 3-10 min. After retraction of the pipette, the pipette tip was placed on the surface of the skull approximately over the site of the injection, and a still image was taken to aid in the subsequent identification of the site of the injection relative to the cortical vasculature. The skin incision was then closed with silk or Vicryl sutures and the animal allowed to recover. Expression time ranged from 14 to 85 days. On the day of the experiment, animals were again anesthetized with ketamine and xylacine (doses and maintenance of anesthesia as above), the skull over somatosensory cortex was again exposed and a headplate for the stabilization of the head under the microscope was attached. After identifying the location of the preceding virus injection, a large craniotomy (approx 2.5 x 2.5 mm) was made, centered on that location and the dura opened. Astrocytes were counterstained stained in some experiments by applying sulforhodamine 101 briefly to the surface of the brain as previously described[18] (Supplementary Fig. 1b) and the preparation was stabilized using agar (1%, Sigma) and a coverslip as described in[7] (note that surface applying sulforhodamine 101 leads to limited depth penetration).

The virus solution was prepared as follows: The enhanced green fluorescent protein (EGFP) open reading frame (ORF) in the pAAV-6P-SEWB vector[36] was substitued by GCaMP3 ORF (802bp)[9], putting GCaMP3 under the control of the human synapsin promoter and stabilizing expression by the woodchuck hepatitis post-transcriptional regulatory element (WPRE). From this pAAV-syn-GCaMP3-WPRE vector a chimeric serotype 1/2 AAV with a genomic titer of 6.5×10^{12} particles/ml was generated using a disontinuous iodixanol density gradient, as described in[37]. Virus purity was verified on a GelcodeTM (Thermo Scientific) stained 12% polyacrylamid gel.

Histology

At the end of the experiment, animals were perfused transcardially with phosphate buffer (PB) followed by 4% paraformaldehyde. The brain was removed and postfixed in PB containing 4% PFA for at least 8 hours. The brain was then cryoprotected by incubation in 30% sucrose solution in PB for 2 to 3 days prior to cutting 100 µm thick coronal sections using a freezing microtome (Mictrom HM440E, Microm, Germany). Slices were mounted, embedded with Vectashild Mounting Medium (Vector Laboratories, CA, USA), covered with a coverslip and sealed with nail polish. Histological images shown in Fig. 1 were obtained using a standard upright light microscope (Axio imager Z1, Zeiss, Germany).

Data analysis

Processing and analysis of raw data was performed using custom written software executed in Matlab (Mathworks, CA, USA) as described previously[13].

Soma/Surround ratio analysis

For calculation of the Soma/Surround ratio, regions of interest (ROIs) were first drawn around individual neuronal somata. The soma signal was calculated frame wise as the mean pixel intensity of the pixels within the ROI. Segments of the data files in which Ca^{2+}-transients exceeded 15% $\Delta F/F0$ were observed were then manually excluded from this analysis, as were segments of the datasets in which stimuli were presented. For each soma ROI, the shape of the ROI was then expanded using a dilatation operation with a

disk shaped structuring element having a 4 pixel radius, and an annulus calculated as the subtraction of the initial ROI from the expanded one. The surround signal was then calculated for each frame as the mean intensity of the pixels in the annulus. The Soma/Surround ratio was then calculated for each frame, and a mean value for all non-excluded imaging frames for each identified neuron calculated.

Analysis of somatic and neuropil-related Ca^{2+}-signal correlation

We estimated neuropil contamination of somata signals by using a linear regression as in previous work[13,24]. For each neuron we first excluded all time points within 0.5 s before or after any fluorescence increase potentially arising from AP discharge (ΔF/F0 at least 1 s.d. above mean), since neuropil fluorescence is known to increase during AP discharge in the local neuronal population[7]. Over the remaining time points we then regressed the observed somatic fluorescence against fluorescence signals measured from nearby neuropil (normalized to give mean 0, s.d. 1) and a constant term. This produced for each neuron a regression coefficient valued in ΔF/F0 indicating the extent to which neuropil signals were present in that neuron, which we termed the neuropil contamination amplitude.

Analysis of stimulus responses

Data were first Gaussian filtered with a width of 0.8ms. For each neuron or dendrite the mean ΔF/F in a 3s window prior to the stimulus and in a 500ms window following each stimulus was calculated. For a given stimulus, if the mean ΔF/F in the post-stimulus

window was greater than the mean + 1 standard deviation of the ΔF/F in the pre-stimulus window, the neuron or dendrite was defined as responding to that stimulus.

References:

1. Denk, W., Strickler, J.H. & Webb, W.W. Two-photon laser scanning fluorescence microscopy. *Science* **248**, 73-76 (1990).
2. Kerr, J.N. et al. Spatial organization of neuronal population responses in layer 2/3 of rat barrel cortex. *J Neurosci* **27**, 13316-13328 (2007).
3. Ohki, K., Chung, S., Ch'ng, Y.H., Kara, P. & Reid, R.C. Functional imaging with cellular resolution reveals precise micro-architecture in visual cortex. *Nature* **433**, 597-603 (2005).
4. Sato, T.R., Gray, N.W., Mainen, Z.F. & Svoboda, K. The functional microarchitecture of the mouse barrel cortex. *PLoS Biol* **5**, e189 (2007).
5. Rothschild, G., Nelken, I. & Mizrahi, A. Functional organization and population dynamics in the mouse primary auditory cortex. *Nat Neurosci* **13**, 353-360 (2010).
6. Dombeck, D.A., Graziano, M.S. & Tank, D.W. Functional clustering of neurons in motor cortex determined by cellular resolution imaging in awake behaving mice. *J Neurosci* **29**, 13751-13760 (2009).
7. Kerr, J.N., Greenberg, D. & Helmchen, F. Imaging input and output of neocortical networks in vivo. *Proc Natl Acad Sci U S A* **102**, 14063-14068 (2005).
8. Hasan, M.T. et al. Functional fluorescent Ca2+ indicator proteins in transgenic mice under TET control. *PLoS Biol* **2**, e163 (2004).
9. Tian, L. et al. Imaging neural activity in worms, flies and mice with improved GCaMP calcium indicators. *Nat Methods* **6**, 875-881 (2009).
10. Wallace, D.J. et al. Single-spike detection in vitro and in vivo with a genetic Ca2+ sensor. *Nat Methods* **5**, 797-804 (2008).
11. Lavis, L.D. & Raines, R.T. Bright ideas for chemical biology. *ACS chemical biology* **3**, 142-155 (2008).
12. Dombeck, D.A., Khabbaz, A.N., Collman, F., Adelman, T.L. & Tank, D.W. Imaging large-scale neural activity with cellular resolution in awake, mobile mice. *Neuron* **56**, 43-57 (2007).
13. Greenberg, D.S., Houweling, A.R. & Kerr, J.N. Population imaging of ongoing neuronal activity in the visual cortex of awake rats. *Nat Neurosci* **11**, 749-751 (2008).
14. Helmchen, F., Svoboda, K., Denk, W. & Tank, D.W. In vivo dendritic calcium dynamics in deep-layer cortical pyramidal neurons. *Nat Neurosci* **2**, 989-996 (1999).
15. Grewe, B.F., Langer, D., Kasper, H., Kampa, B.M. & Helmchen, F. High-speed in vivo calcium imaging reveals neuronal network activity with near-millisecond precision. *Nat Methods* **7**, 399-405 (2010).
16. Mrsic-Flogel, T.D. et al. Homeostatic regulation of eye-specific responses in visual cortex during ocular dominance plasticity. *Neuron* **54**, 961-972 (2007).
17. Stosiek, C., Garaschuk, O., Holthoff, K. & Konnerth, A. In vivo two-photon calcium imaging of neuronal networks. *Proc Natl Acad Sci U S A* **100**, 7319-7324 (2003).
18. Nimmerjahn, A., Kirchhoff, F., Kerr, J.N. & Helmchen, F. Sulforhodamine 101 as a specific marker of astroglia in the neocortex in vivo. *Nat Methods* **1**, 31-37 (2004).

19. Theer, P. & Denk, W. On the fundamental imaging-depth limit in two-photon microscopy. *J Opt Soc Am A Opt Image Sci Vis* **23**, 3139-3149 (2006).
20. Theer, P., Hasan, M.T. & Denk, W. Two-photon imaging to a depth of 1000 microm in living brains by use of a Ti:Al2O3 regenerative amplifier. *Opt Lett* **28**, 1022-1024 (2003).
21. Kerr, J.N. & Denk, W. Imaging in vivo: watching the brain in action. *Nat Rev Neurosci* **9**, 195-205 (2008).
22. Theer, P. in Combined Faculties for the Natural Sciences and for Mathematics, Vol. Doctor of Natural Sciences 100 (University of Heidelberg, Heidelberg; 2004).
23. Oheim, M., Beaurepaire, E., Chaigneau, E., Mertz, J. & Charpak, S. Two-photon microscopy in brain tissue: parameters influencing the imaging depth. *J Neurosci Methods* **111**, 29-37 (2001).
24. Sawinski, J. et al. Visually evoked activity in cortical cells imaged in freely moving animals. *Proc Natl Acad Sci U S A* **106**, 19557-19562 (2009).
25. de Kock, C.P., Bruno, R.M., Spors, H. & Sakmann, B. Layer- and cell-type-specific suprathreshold stimulus representation in rat primary somatosensory cortex. *J Physiol* **581**, 139-154 (2007).
26. Meyer, H.S. et al. Number and laminar distribution of neurons in a thalamocortical projection column of rat vibrissal cortex. *Cereb Cortex* **20**, 2277-2286 (2010).
27. de la Rocha, J., Doiron, B., Shea-Brown, E., Josic, K. & Reyes, A. Correlation between neural spike trains increases with firing rate. *Nature* **448**, 802-806 (2007).
28. Stuart, G.J. & Sakmann, B. Active propagation of somatic action potentials into neocortical pyramidal cell dendrites. *Nature* **367**, 69-72 (1994).
29. Larkum, M.E., Nevian, T., Sandler, M., Polsky, A. & Schiller, J. Synaptic integration in tuft dendrites of layer 5 pyramidal neurons: a new unifying principle. *Science* **325**, 756-760 (2009).
30. Polsky, A., Mel, B.W. & Schiller, J. Computational subunits in thin dendrites of pyramidal cells. *Nat Neurosci* **7**, 621-627 (2004).
31. Stuart, G., Schiller, J. & Sakmann, B. Action potential initiation and propagation in rat neocortical pyramidal neurons. *J Physiol* **505 (Pt 3)**, 617-632 (1997).
32. Margrie, T.W. et al. Targeted whole-cell recordings in the mammalian brain in vivo. *Neuron* **39**, 911-918 (2003).
33. Tsai, P.S. et al. Spherical aberration correction in nonlinear microscopy and optical ablation using a transparent deformable membrane. *Appl. Phys. Lett.* **91** (2007).
34. Ji, N., Milkie, D.E. & Betzig, E. Adaptive optics via pupil segmentation for high-resolution imaging in biological tissues. *Nat Methods* **7**, 141-147 (2010).
35. Rueckel, M., Mack-Bucher, J.A. & Denk, W. Adaptive wavefront correction in two-photon microscopy using coherence-gated wavefront sensing. *Proc Natl Acad Sci U S A* **103**, 17137-17142 (2006).
36. Shevtsova, Z., Malik, J.M., Michel, U., Bahr, M. & Kugler, S. Promoters and serotypes: targeting of adeno-associated virus vectors for gene transfer in the rat

central nervous system in vitro and in vivo. *Experimental physiology* **90**, 53-59 (2005).
37. Zolotukhin, S. et al. Production and purification of serotype 1, 2, and 5 recombinant adeno-associated viral vectors. *Methods (San Diego, Calif* **28**, 158-167 (2002).

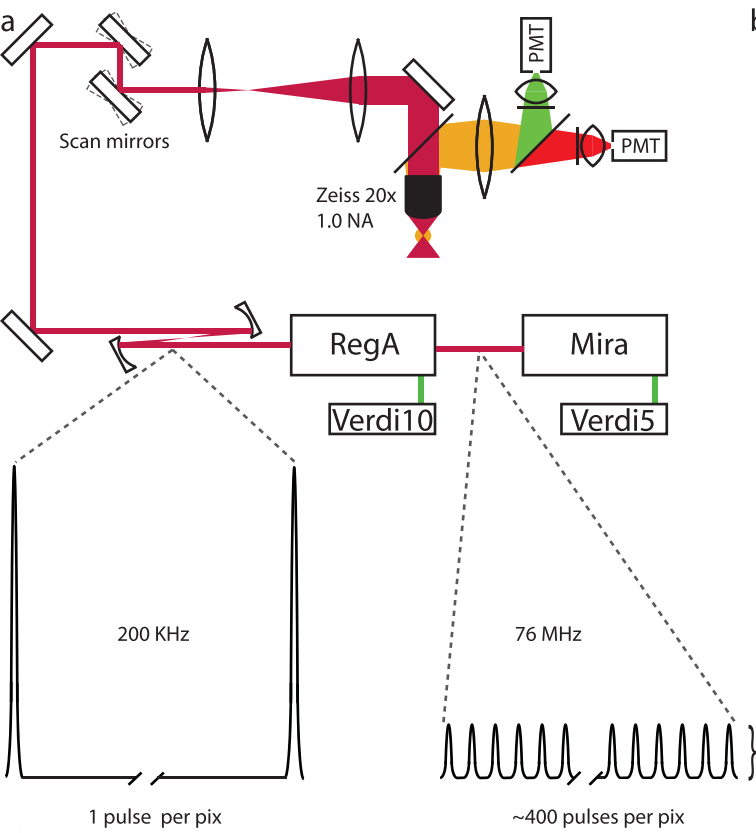

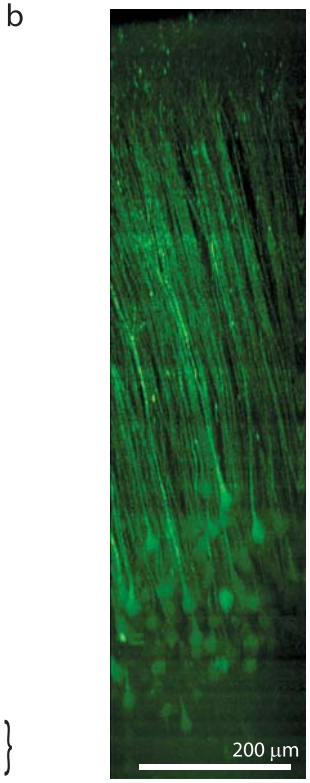

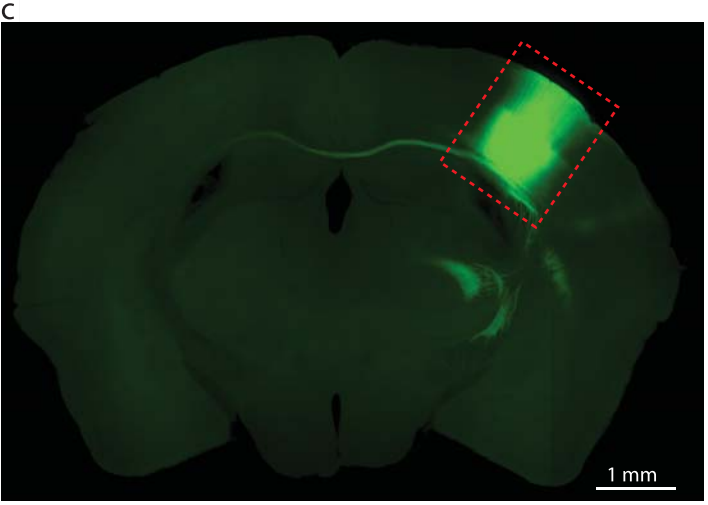

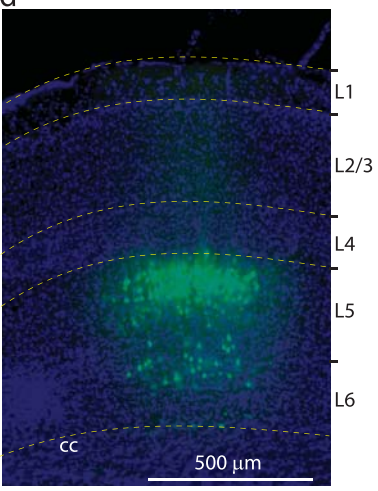

Figure 1

Mittmann_Wallace_Czubayko_Herb_Schaefer_Looger_Denk_Kerr

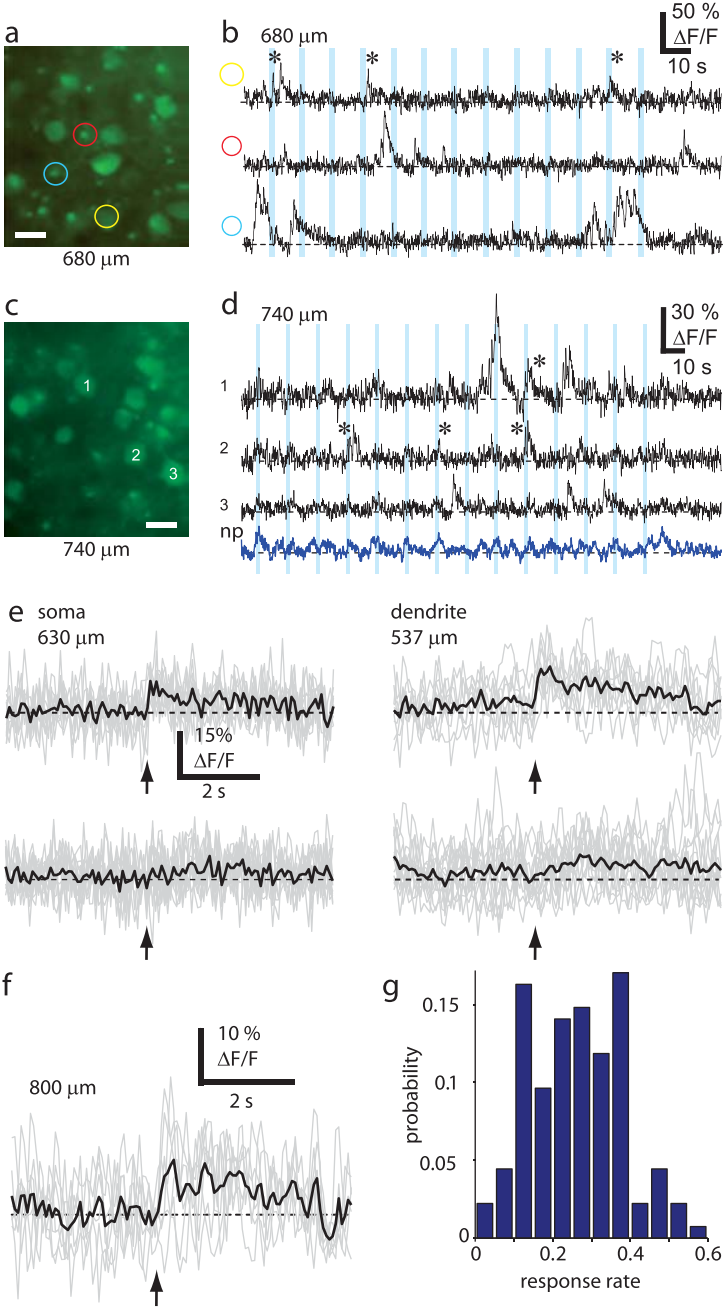

Figure 2

Mittmann_Wallace_Czubayko_Herb_Schaefer_Looger_Denk_Kerr

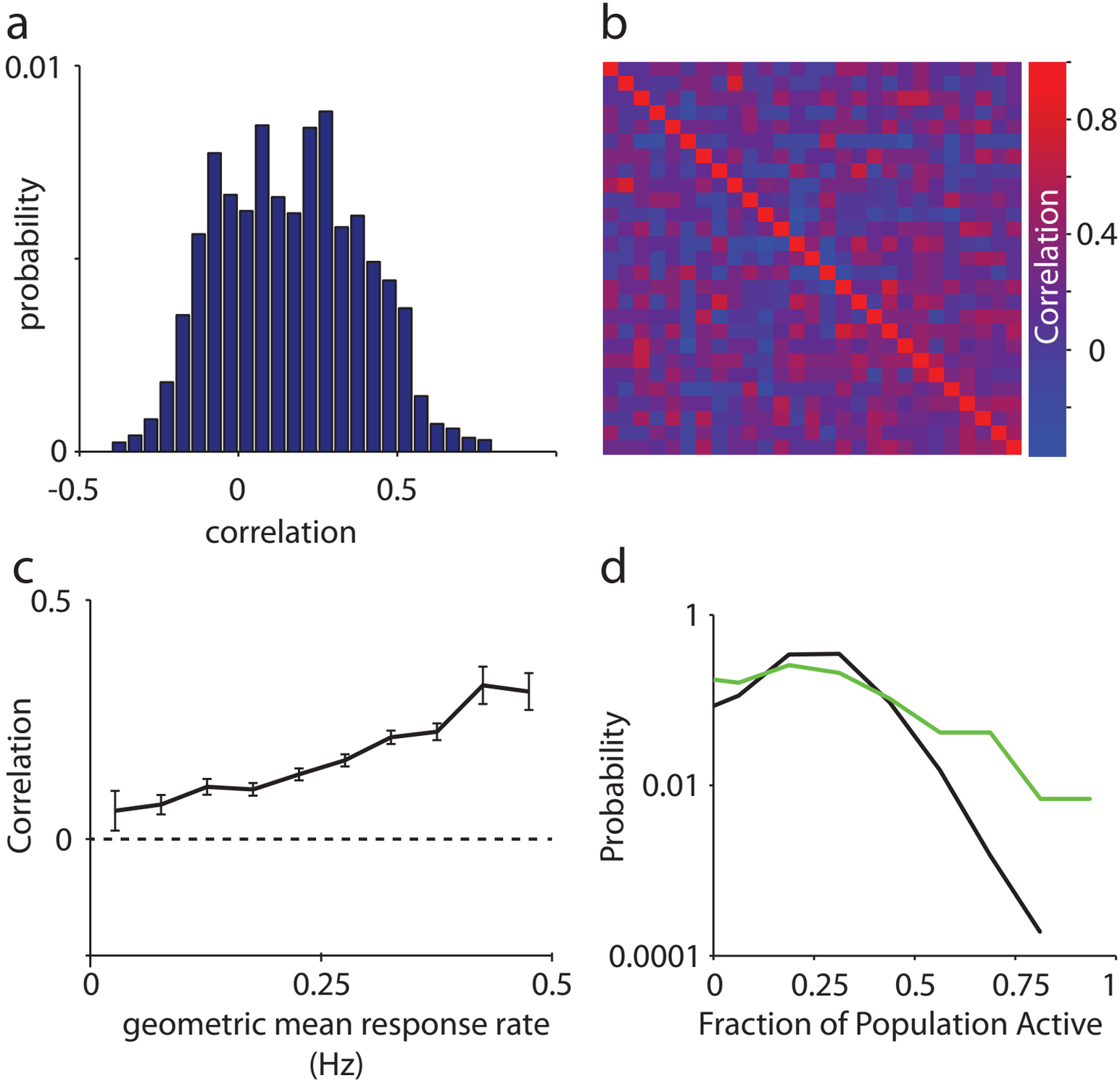
a
0.01
probability
0
-0.5
0
0.5
correlation
b
0.8
0.4
0
Correlation
c
0.5
Correlation
0
0
0.25
0.5
geometric mean response rate
(Hz)
d
1
Probability
0.01
0.0001
0
0.25
0.5
0.75
1
Fraction of Population Active

Figure 3

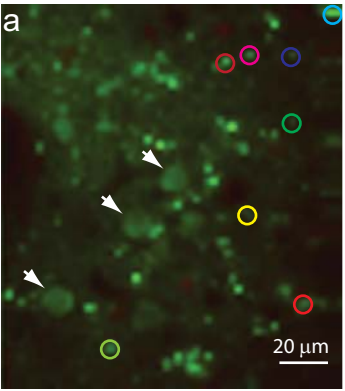

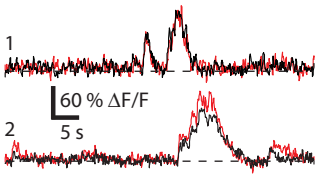

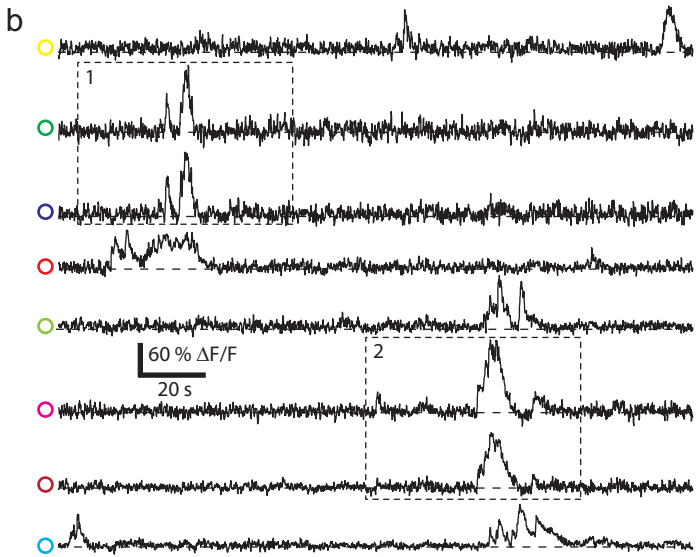

Figure 4

Mittmann_Wallace_Czubayko_Herb_Schaefer_Looger_Denk_Kerr

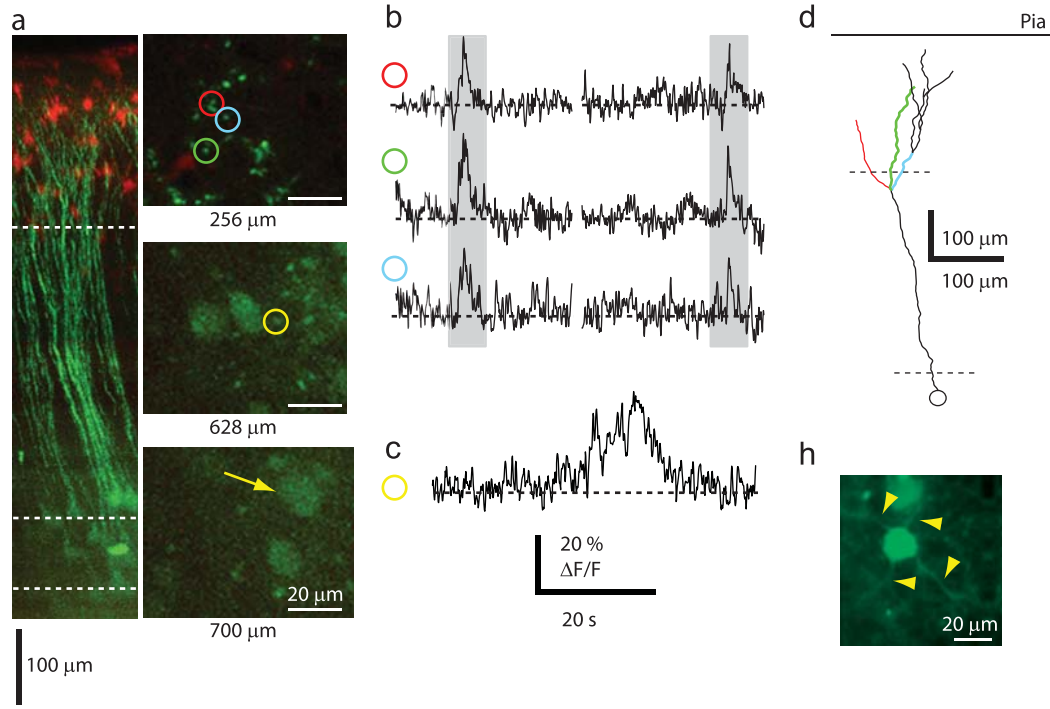

Figure 5

Mittmann_Wallace_Czubayko_Herb_Schaefer_Looger_Denk_Kerr